 doi:10.20944/preprints202010.0014.v1

Type of the Paper (Article)

Enhancement Magneto-optic Properties of Radio-Frequency-Magnetron-sputtered Bi-containing Ferrite Garnet-Type Thin-films using Oxygen Plasma Treatment and Metal-oxide Protective Layers

V. A. Kotov[1], M. Nur-E-Alam[2]*, M. Vasiliev[3], D. E. Balabanov [4], V. I. Burkov[4], and K. Alameh[2],

[1] Institute of Radio Engineering and Electronics, Russian Academy of Sciences, 11 Mohovaya St, Moscow, 125009, Russian Federation; E-mail: kotov.slava@gmail.com (V. A. K.)
[2] Electron Science Research Institute, Edith Cowan University, Joondalup, WA, 6027, Australia; E-mails: m.vasiliev@ecu.edu.au (M. V.), m.nur-e-alam@ecu.edu.au (M.N-E-A.) and k.alameh@ecu.edu.au (K. A.)
[3] Guest Editor for MDPI Applied Sciences, and Sensors, Switzerland; E-mails: vasiliev.mikhail@gmail.com (M. V.)
[4] Moscow Institute of Physics and Technology, 9 Institutski Per., Dolgoprudny, 141700, Russian Federation; E-mails: dima-mipt@mail.ru (D. E. B),
* Correspondence: m.nur-e-alam@ecu.edu.au (M.N-E-A.)

Abstract: Magneto-optic (MO) imaging and sensing are at present the most developed practical applications of thin-film MO garnet materials. However, future component and system-level sensors and imagers technology improvements are still necessary in order to improve sensitivity for a range of established and also the forward-looking applications. These improvements are expected to originate from new material system development. We propose a set of technological modifications for the RF-magnetron sputtering deposition and crystallization annealing of magneto-optic bismuth-substituted iron-garnet films and investigate the improved material properties. Results show that standard crystallization annealing for the as-deposited ultrathin (sputtered 10 nm thick, amorphous phase) films resulted in more than a factor of two loss in the magneto-optical activity of the films in visible spectral region, compared to the liquid-phase grown epitaxial films. Results also show that an additional 10 nm-thick metal-oxide (Bi_2O_3) protective layer above the amorphous film results in ~2.7 times increase in the magneto-optical quality of crystallized iron-garnet films. On the other hand, the effects of post-deposition oxygen (O_2) plasma treatment on the magneto-optical (MO) properties of Bismuth substituted iron garnet thin films material is investigated. Results show that, in the visible part of the electromagnetic spectrum (at 532 nm), the O_2 treated (up to 3 minutes) garnet films retain higher specific Faraday rotation and figure of merit than those of non-treated garnet films.

Keywords: Bi-substituted; magneto-optic; MCD; Faraday rotation; Figure of merit; imaging; sensing; polarization; Oxygen plasma treatment.

1. Introduction

Bismuth (Bi)-substituted garnet materials for various MO applications attracts the attention of researchers in this field to to develop innovative high- performance garnet materials or find ways of improving their properties. Also, from the practical point of view, MO garnet materials of these composition types with high performance are relevant to the context of manufacturing of next-

 doi:10.20944/preprints202010.0014.v1

generation ultra-fast optoelectronic devices, such as light intensity switches and modulators, high-speed flat panel displays, and high-sensitivity sensors [1-14]. Therefore, it is important, nowadays, to obtain MO materials of optimized material composition stoichiometry possessing a high figure of merit and a low coercive field. This can typically be achieved with garnets having high Bi-substitution levels. In recent years, significant research activities have been reported in the field of the manufacture and characterization of a new-generation ultrathin films of yttrium iron garnet (YIG), and related materials, of thicknesses ranging from several nanometers to several tens of nanometers. The record-low optical losses of YIGs in the ultrahigh frequency (UHF) spectral region make them attractive materials for the development of spintronics and modern microwave devices. The low losses of YIGs are due to the small damping parameter $\alpha \approx 3x10^{-5}$ (the ferromagnetic resonance linewidth of less than 0.5 Oe at 9 GHz). Thin films of ferromagnetic metals lag behind YIG materials in performance (in terms of damping characteristics) by two orders of magnitude, thus enabling a significant reduction in switching current for spin valve devices, which are the key components used to develop magnetic sensors, hard disk read heads and magnetic random access memories (MRAM) [1]. Another potential practical area that can benefit from the use of thin YIG films is related to the development of different nano-electronic device types, which utilise the phenomenon of spin current generation by magnetostatic spin waves propagating in thin YIG films possessing small damping parameters [5]. Bismuth-substituted iron garnets, being ferrimagnetic dielectrics possessing giant specific Faraday rotation across the visible and near-infrared spectral regions, also represent the most perspective MO materials for use in different MO devices, such as magnetic photonic crystals (MPC), non-reciprocal MO elements, Faraday-effect ultrafast MO modulators, magnetic field-controlled multilayer MO waveguiding structures, hybrid multiferroics-based multilayers, and other applications in photonics [15-17]. From the point of view of the practical applications of ferrite garnets in hybrid integrated-optics circuits, the most perspective fabrication approach is RF magnetron sputtering of amorphous-phase garnet films onto substrates such as GGG, kept at room temperature (or between 100-400 C), followed by annealing crystallization processes run at temperatures between 490-650 C. The properties of a transitional layer between the substrate and deposited film are a defining factor, which governs the annealing crystallisation process, since the crystallisation processes of these garnet film structures begins from the transitional layer region. When using the thin or ultrathin ferrite garnet layers in bilayer-type structures involving garnet film as spin wave generator and a nanoscale platinum film as spin current detector, at the forefront is the problem of the uniformity of the magnetic properties in thin or ultrathin garnet films, if these also possess record-low damping parameters or small ferromagnetic resonance (FMR) linewidths near 1 Oe. There are literature reports presenting the data showing that in thin and ultrathin iron-garnet films, there exist significant variations in both the composition and magnetic properties across the film thickness [5]. For example, near the substrate-film boundary region, in epitaxially-grown iron garnet films, dependent on growth conditions, complex transitional layers of thickness ranging between several nm up to 250 nm, may form [18]. It is important to note that in these films, the transitional-layer thickness (as evaluated using Curie temperature measurements), may also reach 250 nm. With increasing film thickness, up to 2μm, a constant Curie temperature value is observed.

On the other hand, oxygen plasma treatment is an attractive and widely used technique on both the experimental and industrial scales to improve thin-film technology without having any complexity into the material stoichiometry [19-21]. Oxygen plasma treatment is a well-known method used to clean the substrates for the development of thin films as the oxygen plasma treatment enhances the adhesion of the thin films to the substrates. The optimized oxygen plasma treatment can enhance the thin film's bonding strength (surface energy) and adequately modify the film surfaces for various microelectronics and optoelectronics devices without affecting the entire nanostructures of the devices [19-24]. J. W. Roh et al. have reported that the oxygen plasma assisted wafer bonding process is very effective and crucial for the fabrication of integrated optical waveguide isolators. They treated the surfaces of GGG substrates by oxygen plasma for 30 seconds with a radio frequency (RF) plasma power of 100 W under oxygen pressure of 0.3 Torr, and observed high bonding strength and hydrophilicity without any voids in the interface in bonding of Indium

 doi:10.20944/preprints202010.0014.v1

phosphide (InP) thin films to $Gd_3Ga_5O_{12}$ (GGG) substrates [23]. K. H. Chen et al. have applied the oxygen plasma treatment process in low temperature environment to improve the electrical and physical properties of as-deposited $(Ba_{0.7}Sr_{0.3})(Ti_{0.9}Zr_{0.1})O_3$ (BSTZ) thin films [24]. They have reported that the oxygen plasma treatment affects the chemical bonding state and crystalline structure help reducing the interface states, oxygen vacancies and defects for as-deposited BSTZ thin films, and enhance the capacitance of the films. Growing high-quality thin films of various oxide and metal-oxide materials, including MO garnets, on various substrates, is typically accomplished by creating oxygen plasma and allowing extra oxygen input with argon (Ar), Nitrogen (N_2), or Hydrogen (H) or Helium (He) plasma during the deposition process [25-34]. However, to our knowledge, using post-deposition oxygen plasma treatment on as-deposited highly Bi-substituted iron garnet thin-films, prior to the annealing crystallization processes, has never been reported.

To improve the properties of highly Bi-substituted metal doped iron garnet thin film materials, we propose two new and modified process sequences for annealing crystallization of garnet thin-films. The new method for the manufacture of high-performance ultrathin garnet films is the provision of a thin (2-20 nm) protective bismuth oxide (Bi_2O_3) layer, which assists in the crystallization of the garnet layer. In this case, during the initial stage, a 20-60 nm amorphous-phase film of a nanocomposite material type of ($Bi_2Dy_1Fe_4Ga_1O_{12} + Bi_2O_3$), is deposited onto a gadolinium gallium garnet (GGG), or a glass substrate. The excess bismuth oxide content relative to the stoichiometric composition of ferrite garnet is kept between 10-40 vol %. The second stage involves the deposition (also by RF sputtering) of a protective bismuth-oxide layer of thickness between 2 nm-40 nm onto these amorphous nanocomposite films. The obtained two-layer structure is then subjected to annealing crystallization in air atmosphere, at a temperature between 490°C and 650°C, for 1h. Results show that the MO performance characteristics of the sample (nanocomposite material of composition type $Bi_2Dy_1Fe_4Ga_1O_{12} + Bi_2O_3$ with a protective Bi_2O_3 layer) exceeds, by more than a factor of two, the corresponding parameters obtained in identical material systems fabricated without this additional protective layer. We also report on the studies of the Faraday rotation and its dispersion (conducted in the 400 nm-600 nm interval), as well as the magnetic circular dichroism (MCD, performed in between 300 nm-600 nm). Results demonstrate a two-fold improvement in the MO characteristics of oxide-protected garnet films, due to both the increased bismuth substitution levels, and the prevention of bismuth evaporation from the subsurface film regions.

Secondly, we apply oxygen plasma treatment on as-deposited garnet samples right after deposition and then follow conventional temperature annealing processes to crystallize the garnet thin films. We particularly investigate the effects of post-deposition oxygen plasma treatment on the MO properties of RF sputtered garnet thin-film layers, synthesized using two different types (Bi-contained garnet) of sputtering targets. The oxygen plasma treated and non-treated garnet thin films (after optimally annealed) are characterized and analyzed. In the conducted experiments, we repeatedly noticed that the post-deposition low temperature oxygen plasma significantly interacts with the material layers and improves their materials properties especially the Faraday rotation per film thickness and optical absorption coefficients, thus leading to a high MO figure of merit compared to that of non-treated annealed garnet layers.

2. Background

When using a single solution-melt, depending on the epitaxial growth temperature and the supercooling magnitude, the transitional layer thickness can vary widely, from 5 nm to around 250 nm, with the transitional layer being possibly composed of several intermediate layers. For example, a growth regime with bismuth-containing solution-melt supercooling near ΔT~150 °C at a growth temperature around 750 °C leads to the appearance of an intermediate transitional sublayer of thickness around 100 nm at the substrate-film boundary (Curie temperature of the iron garnet composition being 225 °C). As a result, in this thickness interval, the epitaxial growth process occurs under the conditions that the growth rate being limited by the crystallization rate at the substrate-film boundary. Past this stage, a thick transitional sublayer appears, of thickness near 150 nm, within which the Curie temperature reduces from 225 °C to 215 °C. At the same time, for the material, the

Preprints (www.preprints.org) | NOT PEER-REVIEWED | Posted: 1 October 2020 doi:10.20944/preprints202010.0014.v1

effective field of the uniaxial magnetic anisotropy, defined as $H_k^{eff} = H_k - 4\pi M_s$, changes smoothly from H_k^{eff} = 1500 Oe at the epitaxial layer thickness h = 30 nm, to H_k^{eff} = 2100 Oe, at h = 250 nm. Studies of the lattice parameter dependency on the epitaxial layer thickness conducted in the thickness range between 250 nm and 1mm for Bi-substituted ferrite garnet films showed that both the Curie temperature of material and the lattice parameter do not change, and are equal to Tc = 215 °C and a_f = 12.401 Å, respectively. Within the starting region of the transitional layer, the corresponding measured values were Tc = 225 °C and a_f = 12.412 Å, respectively. According to the data reported in [5], an increase in the Bi substitution by 1 formula unit (f.u.) within epitaxial films has led to an increase in the garnet lattice parameter by Δa_f = 0.0828 Å. Therefore, increasing the Bi-substitution from 0.3 f.u. to 1.43 f.u. should lead to an increase of the lattice parameter from a_f = 12.401 Å to a_f = 12.412 Å, and hence, the data on the T_c and lattice parameter near the film-substrate boundary do not match well.

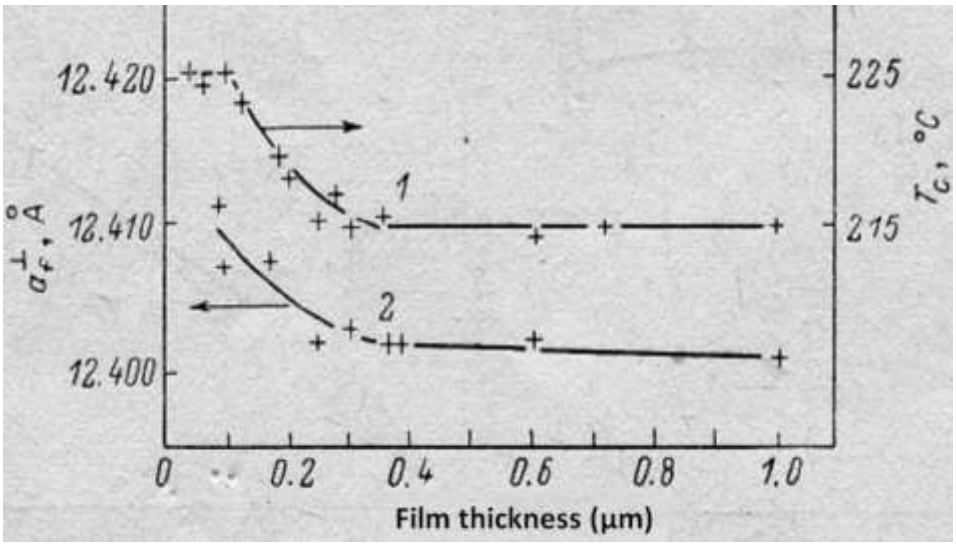

Figure 1. Curie temperature dependency (1) and lattice parameter (2) on epitaxial layer thickness.

At a growth temperature around 980 °C and solution melt supercooling of around ΔT = 5 °C, it is possible to grow an epitaxial garnet layer of thickness around several microns, within which the Curie temperature remains practically constant across the entire volume of the epitaxial layer. It is important to note that, when fabricating thin and ultrathin bismuth-substituted iron-garnet layers, the formation of transitional layers near the film-substrate boundary may also take place due to the partial amorphization of the substrate surface occurring during the pre-deposition argon-plasma bombardment as a result of additional substrate-cleaning measures. The Ar^+ ion energies may, in this case, reach between tens of eV to several keV. Another cause of the significant changes in the composition of film with thickness, and the related changes in the magnetic properties of films, is the annealing crystallization procedure, which takes place within the (composition-dependent) temperature range from 490 C to 650C. Etching of GGG substrates undertaken prior to the epitaxial film growth leads, at best, to the RMS surface roughness of the substrate surface being near ~0.25 nm. Usually, in LPE-grown iron garnet films fabricated while keeping constant melt temperature during growth, a significant reduction of the Bi substitution content is observed across the film layer thickness, towards the direction of the film-air boundary. During the experiments aimed at finding the optimum temperature of epitaxial growth, it has been found that, at a growth temperature between 950°C and 980 °C and melt supercooling near ΔT = 5 – 10 °C, it is possible to manufacture films with constant Curie temperature, within ΔT_c = 3 °C. In this study, several batches of Bi-containing thin-ferrite garnet-type films are fabricated and characterized in order to better understand the annealing crystallization processes for the synthesis Bi-substituted ferrite garnets (which initially are found to be in an amorphous phase after RF magnetron deposition).

3. Garnet layers sputter-deposition and annealing process and parameters

Preprints (www.preprints.org) | NOT PEER-REVIEWED | Posted: 1 October 2020 doi:10.20944/preprints202010.0014.v1

Multiple batches of single-layer bismuth-substituted garnet compounds doped with dysprosium and gallium, and bi-layer structures (garnet layer plus top thin protective oxide layer) have been prepared on glass and monocrystalline garnet substrates using the RF magnetron sputtering technique. The sputtering targets used have nominal compositions of $Bi_2Dy_1Fe_4Ga_1O_{12}$, $Bi_{2.1}Dy_{0.9}Fe_{3.9}Ga_{1.1}O_{12}$, $Bi_{1.8}Lu_{1.2}Fe_{3.6}Ga_{1.4}O_{12}$, and Bi_2O_3. From our previous work, we had found that the films of co-sputtered composition type ($Bi_2Dy_1Fe_4Ga_1O_{12}$ sputtered with excess Bi_2O_3) possesses simultaneously a high Faraday rotation and the necessary level of uniaxial magnetic anisotropy to orient the magnetization of the films in the direction perpendicular to the film plane.

Some of as-deposited garnet layers were treated with oxygen plasma exposure immediately after the deposition process before the high temperature crystallization process was performed. The process parameters used to prepare the garnet layers, including sputter deposition, oxygen plasma exposer and annealing crystallization, are detailed in Table 1. O_2 plasma treatment was conducted using YZD08-5C plasma cleaner for 0.5-5 minutes. The plasma-treated and the non-treated samples were then annealed by using the optimized annealing regimes found in previous annealing experiments for this composition of garnet layers [3, 4]. The film quality and the properties of annealed garnet samples were first characterized in terms of the specific Faraday rotation and MO figure of merit at 532 nm.

In this work, the post-deposition annealing processes were run using a conventional temperature-controlled and heating-rate-controlled oven in the temperature range of 490 to 650 °C.

Table 1. Summary of process parameters used to prepare the garnet layers.

Sample preparation stage	**Process parameters**	**Values & Comments**
Garnet layers deposition	Sputtering target stoichiometry oxide-mixed garnet targets	$Bi_2Dy_1Fe_4Ga_1O_{12}$, $Bi_{2.1}Dy_{0.9}Fe_{3.9}Ga_{1.1}O_{12}$, $Bi_{1.8}Lu_{1.2}Fe_{3.6}Ga_{1.4}O_{12}$, and Bi_2O_3
	Base pressure (Torr)	$4\text{-}5 \times 10^{-6}$
	Argon (Ar) pressure	≈ 2 mTorr
	Substrate stage temperature (°C)	Room Temperature (21-23 °C)
	Substrate stage rotation rate (rpm)	33-34
Oxygen plasma treatment	Base pressure	100 Pa
	Oxygen flow	0.2 sccm/min
	RF power densities	40 W
	Plasma exposure time	30 sec to 5 minutes

Several batches of simple (double and triple)-layer-type all-garnet heterostructures were also manufactured, investigated and their optimized process parameters and properties (i.e., optimizing the heterostructure annealing regimes and characterizing the crystallization behavior, inter-material compatibility and microstructural properties) were reported by our group. Our previously published data confirmed the annealing crystallization of behavior of Bi-substituted iron garnet and garnet-oxide composites deposited onto various substrate types [3-5, 35, 36].

4. Results

4.1. Spectral dependencies of Faraday rotation measured for nanocrystalline films of composition $Bi_2Dy_1Fe_4Ga_1O_{12}$

Figure 2 shows the spectral dependency of the specific Faraday rotation, where a peak at 494 nm is observed, for a $Bi_2Dy_1Fe_4Ga_1O_{12}$ film of around 150 nm thickness. When measuring the MO characteristics in samples of less than 20 nm thickness, across the temperature interval between 8K – 200K, we observed magnetic circular dichroism (MCD) spectra similar to these typical for

Preprints (www.preprints.org) | NOT PEER-REVIEWED | Posted: 1 October 2020 doi:10.20944/preprints202010.0014.v1

nanocrystalline Bi-substituted ferrite garnets with thicknesses between 500-1000 nm. During this study, we measured the MCD spectra between 250-600 nm.

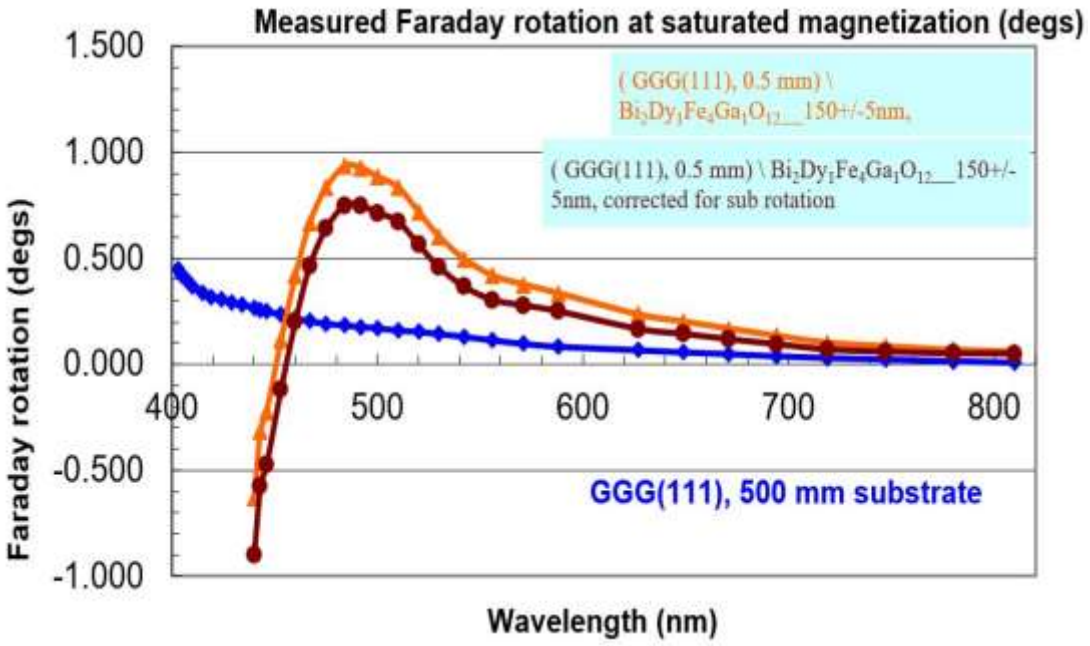

Figure 2. Spectral dependencies of Faraday rotation measured for nanocrystalline films of composition $Bi_2Dy_1Fe_4Ga_1O_{12}$ at saturated magnetization stage.

Y. Sun et al. has reported PLD-manufactured YIG films on GGG substrates with FMR linewidth of 3.4 Oe, defined as the interval between the extrema of the derivative of the FMR absorption line at 10 GHz. The film surface roughness determined by scanning probe microscopy was between 1-3 nm [37]. The years 2010 and 2011 witnessed the birth of a new paradigm in the discipline of spintronics—"spintronics using yttrium iron garnets [1, 15-17, 38]. The significance of this research field originates from two features of yttrium iron garnet (Y3Fe5O12, YIG) materials: (1) extremely small damping factor, and (2) electrically-insulating property.

4.2. Scpectral dependencies of magnetic circular dichroism for standard nanocomposite-type samples of $Bi_2Dy_1Fe_4Ga_1O_{12} + Bi_2O_3$

In this study, we measured the magnetic circular dichroism (MCD) spectra in the wavelength range of 250 - 600 nm in nanocomposite films of bismuth-containing ferrite garnets with an excess of bismuth oxide. The results of studying the spectral dependence of magnetic circular dichroism in a nanocomposite film of the $Bi_2Dy_1Fe_4Ga_1O_{12} + Bi_2O_3$ system in the spectral range from 250 to 600 nm are shown in Fig. 3. The sign of the MCD effect is opposite to the sign of MCD observed in films of ferrite garnets of composition $(YBi)_3Fe_5O_{12}$ [36]. This is because the studied sample has a magnetic compensation point at a temperature above room temperature. Note that, for $(YBi)_3Fe_5O_{12}$ samples, the tetrahedral magnetic sublattice of a ferrite garnet is oriented along the applied magnetic field, however, by the substituting yttrium ions by dysprosium ions and iron ions by gallium ions in the dodecahedral ferrite garnet sublattice reverses the magnetization orientation.

Preprints (www.preprints.org) | NOT PEER-REVIEWED | Posted: 1 October 2020 doi:10.20944/preprints202010.0014.v1

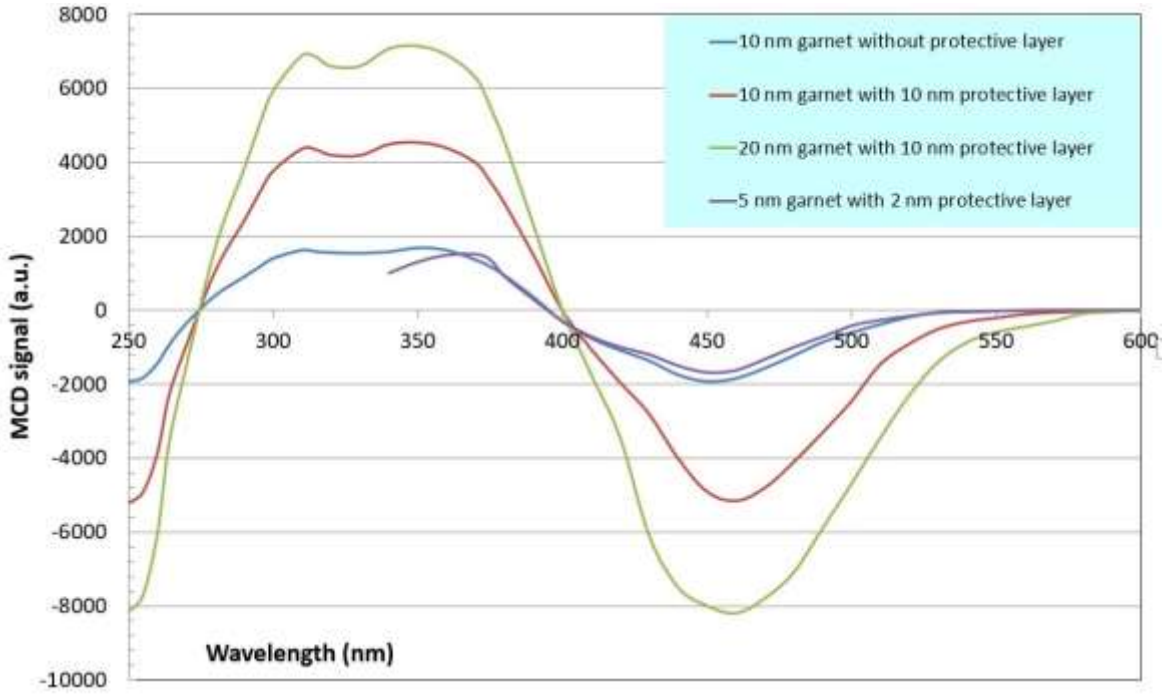

Figure 3. Spectral dependences of the magnetic circular dichroism of ferrite garnet films, deposited using$Bi_2Dy_1Fe_4Ga_1O_{12}$ + Bi_2O_3 targets, in the spectral range from 250 to 600 nm, crystallized without a protective layer (row 1, film thickness 10 nm) and under a protective layer Bi_2O_3 (row 2, film thickness 10 nm, protection 5 nm Bi_2O_3; row 3, film thickness 20 nm, protection 5 nm Bi_2O_3; row 4, thickness 5 nm, protection 2 nm Bi_2O_3, spectral range 340 - 600 nm).

4.3 $Bi_{2.1}Dy_{0.9}Fe_{3.9}Ga_{1.1}O_{12}$ and $Bi_{1.8}Lu_{1.2}Fe_{3.6}Al_{1.4}O_{12}$ garnet layers annealled followed by post-deposition oxygen plasma treatment

XRD traces obtained for as-deposited and annealed $Bi_{2.1}Dy_{0.9}Fe_{3.9}Ga_{1.1}O_{12}$ films using a Siemens 5000D x-ray diffractometer are shown in Fig. 4. The presence of weak broad hump at ~38.2° in the XRD pattern of the as-deposited garnet samples is attributed to the amorphous phase of the samples just after deposition as well as to the post oxygen plasma exposure. However, following annealing at 580 °C, the broadened hump at 38.2° is turned into a small, but significantly noticeable, peak (512) together with a number of stronger peaks consistent with the primary garnet phase representing their crystallization stage and the nanocrystalline microstructure of the garnet films. All identified XRD peaks and their angular positions with the half maximum-line width (FWHM) values were determined using Jade 9 (MDI Corp.) software package (Peak-listing option). The lattice constant and crystallite sizes for the synthesized garnet-type materials were calculated using the standard procedures followed in Ref [3].

Preprints (www.preprints.org) | NOT PEER-REVIEWED | Posted: 1 October 2020 doi:10.20944/preprints202010.0014.v1

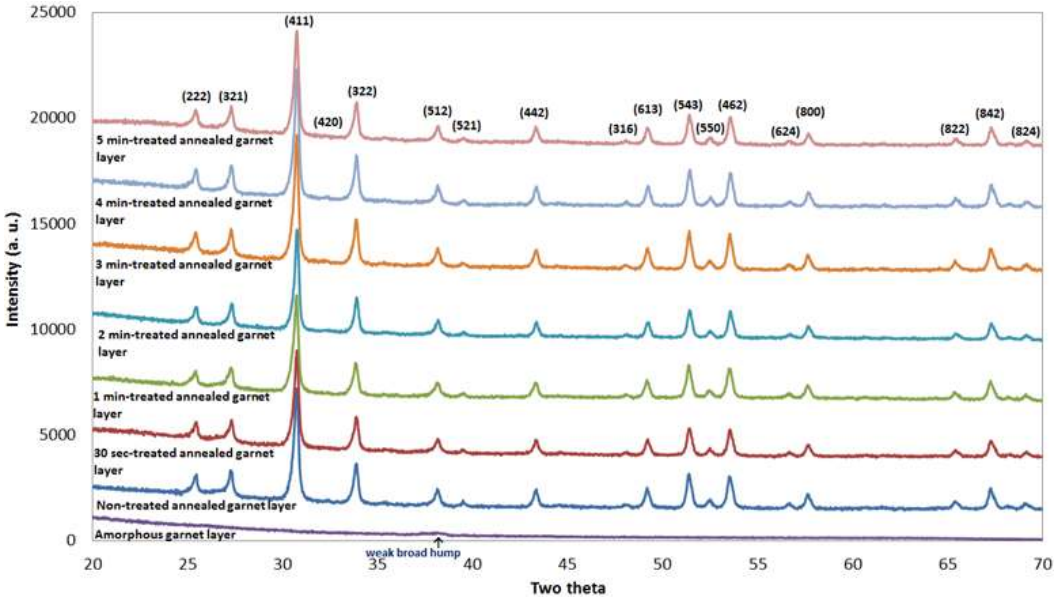

Figure 4. Measured XRD patterns in as-deposited and annealed $Bi_{2.1}Dy_{0.9}Fe_{3.9}Ga_{1.1}O_{12}$ garnet layers.

To investigate the effects of post-deposition oxygen plasma treatment on the optical and magneto-optical behaviours of $Bi_{2.1}Dy_{0.9}$IG type thin films, we derived the optical absorption coefficients, measured the specific Faraday rotation and calculated the MO figure of merit at a certain spectral wavelength (532 nm). The transmission spectra of all annealed garnet layers were spectrally fitted with the modeled transmission spectra to determine the optical absorption on the garnet layers by using the MPC software reported in [39]. The plasma-treated samples showed slightly higher specific Faraday rotation at 532 nm compared to the non-treated garnet samples, and this was repeatedly observed in all batches of plasma treated annealed samples. However, significantly lower optical losses (optical absorption) were observed in the O2-plasma-treated (up to 3 minutes) garnet layers than that of non-treated garnet films, thus leading to an improved MO figure of merit ($Q = 2 \times \Theta_F/\alpha$, where Θ_F is the specific Faraday rotation and α is the absorption coefficients) as shown in Fig. 5. Estimated errors in films' thicknesses (within ± 5% accuracy) as well as in Faraday rotation were accounted for during the calculations of the MO figures of merit.

Preprints (www.preprints.org) | NOT PEER-REVIEWED | Posted: 1 October 2020 doi:10.20944/preprints202010.0014.v1

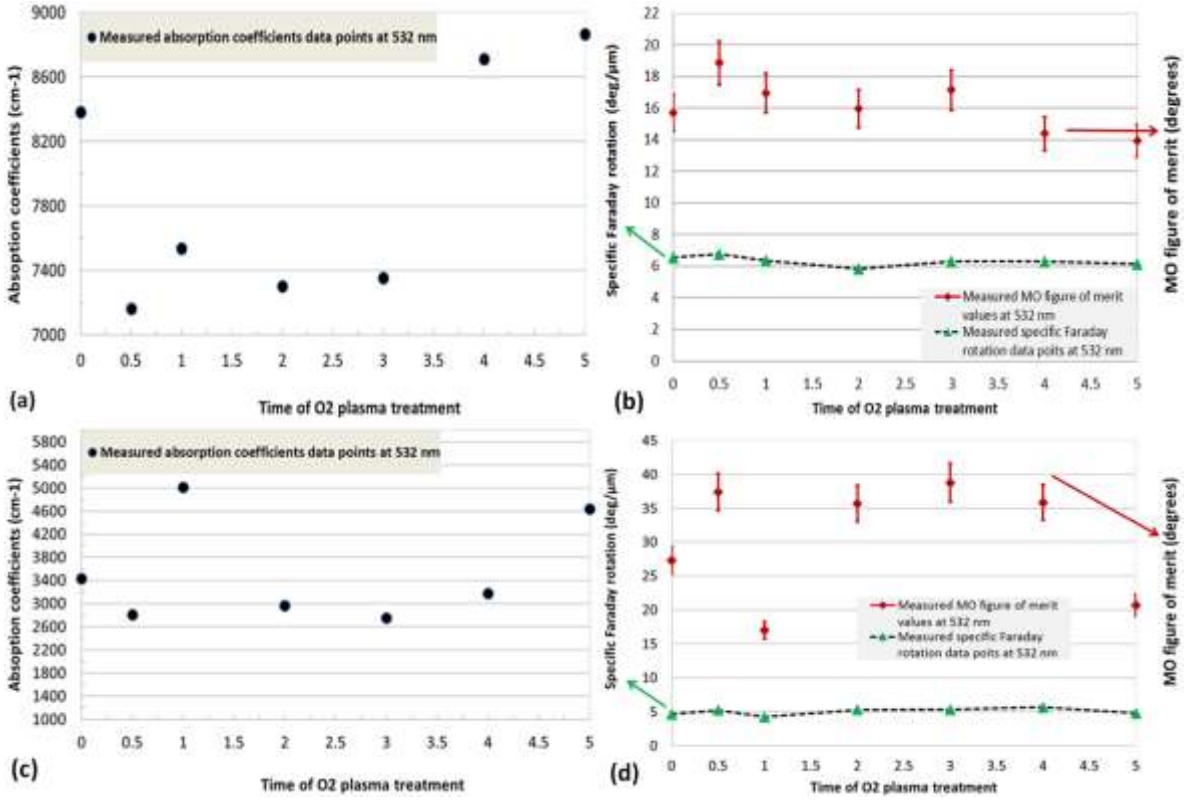

Figure 5. Measured optical absorption coefficients, specific Faraday rotation and MO figure of merit data points at 532 nm in optimally annealed O2 plasma treated and non-treated $Bi_{2.1}Dy_{0.9}Fe_{3.9}Ga_{1.1}O_{12}$ and $Bi_{1.8}Lu_{1.2}Fe_{3.6}Al_{1.4}O_{12}$ garnet layers.

The best MO properties were obtained in the sample that was exposed to oxygen plasma for only 30 seconds inside the high vacuum chamber. This sample showed highest specific Faraday rotation, lowest optical absorption at 532 nm. The highest MO figure of merit, about 19 degrees, was obtained in the 30-second plasma-treated garnet layer of composition type $Bi_{2.1}Dy_{0.9}Fe_{3.9}Ga_{1.1}O_{12}$ whilst the highest MO figure of merit, above 35 degrees, was obtained in plasma-treated garnet layers of composition type $Bi_{1.8}Lu_{1.2}Fe_{3.6}Al_{1.4}O_{12}$. It is important to note that the specific Faraday rotation slightly decreased with increasing the plasma treatment time, however, the absorption coefficient increased significantly with the plasma exposure time, and, consequently, reduced the MO quality of the garnet layers after 3 minutes.

The surface roughness profile of the garnet thin films (oxygen plasma treated and non-treated) were studied, and it was found that all annealed samples exhibited smooth, uniform and consistent morphology across film surfaces except some minor microcracks (occurred due to substrates high temperature expansion and also for the lattice mismatch of the garnet layer and the substrate). Garnet films exposed to oxygen plasma for 30 seconds possessed the best surface quality with RMS roughness value (Rq) of around 0.5 nm. This indicates that such films have a significant surface effects while other samples including the non-treated garnet layer showed RMS value over 1nm. From the above discussion it can be concluded that the O_2 plasma treatment effectively interacts with the material surface layer and reduces the surface roughness without intruding into the entire layer structure. This changes the surface energy of the garnet layers and helps the garnet layers get more oxygen diffusion during the annealing crystallization process, leading to better MO properties compared to the non-treated garnet layers. Note that, films treated with O_2 plasma for longer than 30 s displayed surface larger nanoscale grain features (Fig. 6).

Preprints (www.preprints.org) | NOT PEER-REVIEWED | Posted: 1 October 2020 doi:10.20944/preprints202010.0014.v1

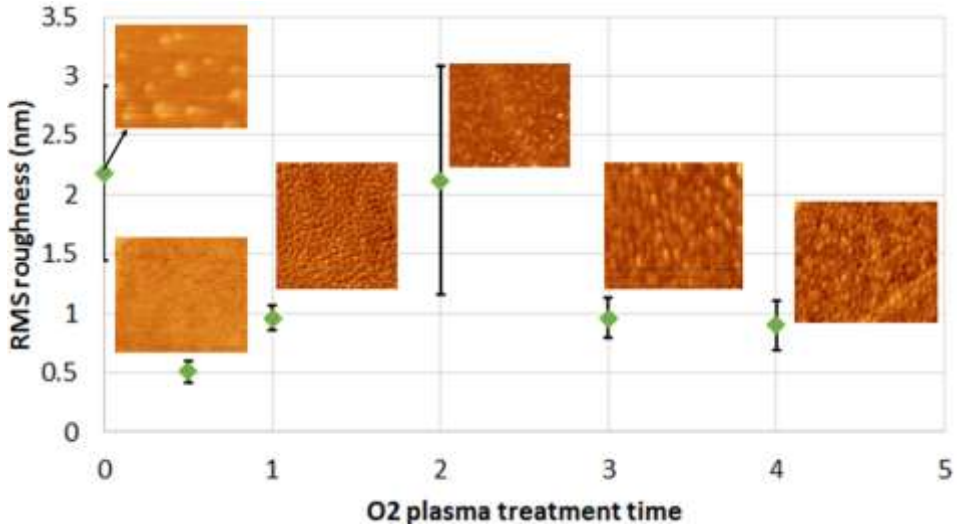

Figure 6. AFM images and measured rms surface roughness values vs oxygen plasma exposure time, for the various developed garnet thin films.

The AFM images shown in Fig. 6 () reveal that all lasma-treated garnet films exhibit a very homogeneous distribution of grains and that their grain shape is nearly spherical (Fig 7). A slight change in grain shape, from spherical to irregular, is observed in the garnet films treated by the O_2-plasma more than 30 seconds. However, it was observed that the MO figure of merit decreased with the increase in plasma treatment time though the specific Faraday rotation remained higher compared to that of the non-treated annealed garnet layer. This is an ongoing research work and will be continued in order to develop new garnet materials with improved MO properties for existing and emerging applications in magneto photonic, magneto-plasmonic and integrated optics.

5. Conclusions

Studies of the magneto-optical properties of ultrathin RF magnetron sputtered bismuth-substituted iron garnet films of thickness between 2.5-20 nm have been conducted in the temperature interval from room temperature down to 8K. For the first time, the effects of thin protective Bi_2O_3 layers on the MO properties of ultrathin highly bismuth-substituted dysprosium iron garnet layers have been investigated. At room temperature, and also at cryogenic temperatures, the spectral dependencies of magnetic circular dichroism have been measured between 250-850 nm. At room temperature, the MCD spectra typical of Bi-substituted ferrite garnets have been measured (in samples without protective oxide layers), in films of thickness 10.3 nm and above.

In order to improve the MO quality in ultrathin nanocomposite films of co-sputtered composition type $Bi_2Dy_1Fe_4Ga_1O_{12}$ + Bi_2O_3, we have introduced a new modification of the annealing crystallization process, in which a 10 nm-thick protective layer of Bi_2O_3 served to prevent the films from Bi content loss otherwise occurring during the high-temperature annealing. Results show that the magnitude of MCD signal measured at 450 nm in oxide-protected annealed film of system $Bi_2Dy_1Fe_4Ga_1O_{12}$ + Bi_2O_3, is 2.7 times higher than that of a $Bi_2Dy_1Fe_4Ga_1O_{12}$ unprotected by an oxide layer. The properties of the garnet thin films can also be improved by employing the oxygen plasma treatment just after the deposition process.

Author Contributions: "Conceptualization, V.A.K.; M.N.-E-A. and M.V.; methodology, V.A. K.; M.N.-E-A. and M.V.; software, M.V.; M.N.-E-A. and K.A.; validation, V.A.K.; M.N.-E-A.; M.V.; D.E.B.; V.I.B. and K.A.; formal analysis, V.A.K.; M.N.-E-A. and M.V.; investigation, V.A.K.; M.N.-E-A. and M.V.; data curation, V.A.K.; M.N.-E-A. and M.V.; writing—original draft preparation, V.A.K.; M.N.-E-A. and M.V.; writing—review and editing, V.A.K.; M.N.-E-A.; M.V.; D.E.B V.I.B. and K.A.; visualization, V.A.K.; M.N.-E-A.; M.V.; D.E.B.; V.I.B. and K.A. All authors have read and agreed to the published version of the manuscript.

Funding and Acknowledgement: This research is partially supported by the Electron Science Research Institute, Edith Cowan University, Australia. Also this study is supported by a grant from the Russian Foundation for Basic Research (project RFBR 19-07-00444 A) at the Institute of Radio Engineering and Electronics named after V.A. Kotel'nikov, Russian Academy of Sciences (the process of crystallization annealing of thin and ultrathin films of ferrite garnets was tested), as well as RFBR grant (project 19-07-00408 A) the Russian Foundation for Basic Research (project 19-07-00444 A) at Moscow Physical-technical institute (Moscow Institute of Physics and Technology (studies of the optical and magneto-optical properties of experimental samples of films of bismuth-containing ferrite garnets).

Studies of the magneto-optical properties of ultrathin films of bismuth-containing ferrite garnets on gadolinium-gallium garnet substrates with thicknesses of 0.7, 1.7, and 3.7 nm were carried out with the support of the state budget.

received no external funding.

Conflicts of Interest: The authors declare no conflict of interest.

References

1. Zvezdin, A.K.; Kotov, V.A. *Modern Magnetooptics and Magnetooptical Materials*;
2. Sylgacheva, D.; Khokhlov, N.; Kalish, A.; Dagesyan, S.; Prokopov, A.; Shaposhnikov, A.; Berzhansky, V.; Nur-E-Alam, M.; Vasiliev, M.; Alameh, K.; et al. Transverse magnetic field impact on waveguide modes of photonic crystals. *Optics Letters* **2016**, *41*, 3813, doi:10.1364/OL.41.003813.
3. Nur-E-Alam, M.; Vasiliev, M.; Alameh, K. High-performance RF-sputtered Bi-substituted iron garnet thin films with almost in-plane magnetization. *Optical Materials Express* **2017**, *7*, 676, doi:10.1364/ome.7.000676.
4. Nur-E-Alam, M.; Vasiliev, M.; Kotov, V.A.; Alameh, K. Highly bismuth-substituted, record-performance magneto-optic garnet materials with low coercivity for applications in integrated optics, photonic crystals, imaging and sensing. *Optical Materials Express* **2011**, *1*, 413, doi:10.1364/ome.1.000413.
5. Vasiliev, M.; Alam, M.N.-E.; Kotov, V.A.; Alameh, K.; Belotelov, V.I.; Burkov, V.I.; Zvezdin, A.K. RF magnetron sputtered (BiDy)_3(FeGa)_5O_12:Bi_2O_3 composite garnet-oxide materials possessing record magneto-optic quality in the visible spectral region. *Optics Express* **2009**, *17*, 19519, doi:10.1364/OE.17.019519.
6. Kuz'michev, A.; Kreilkamp, L.; Nur-E-Alam, M.; Bezus, E.; Vasiliev, M.; Akimov, I.; Alameh, K.; Bayer, M.; Belotelov, V. Tunable Optical Nanocavity of Iron-garnet with a Buried Metal Layer. *Materials* **2015**, *8*, 3012–3023, doi:10.3390/ma8063012.
7. Nur-E-Alam, M.; Vasiliev, M.; Kotov, V.; Balabanov, D.; Akimov, I.; Alameh, K. Properties of Exchange Coupled All-garnet Magneto-Optic Thin Film Multilayer Structures. *Materials* **2015**, *8*, 1976–1992, doi:10.3390/ma8041976.
8. Hibiya, T.; Morishige, Y.; Nakashima, J. Growth and Characterization of Liquid-Phase Epitaxial Bi-Substituted Iron Garnet Films for Magneto-Optic Application. *Japanese Journal of Applied Physics* **1985**, *24*, 1316–1319, doi:10.1143/JJAP.24.1316.
9. Huang, M.; Zhang, S. A New Bi-substituted Rare-earth Iron Garnet for a Wideband and Temperature-stabilized Optical Isolator. *Journal of Materials Research* **2000**, *15*, 1665–1668, doi:10.1557/JMR.2000.0240.
10. Zeazjev, M. Magneto-optic iron-garnet thin films for integrated optical applications. *SPIE Newsroom* **2007**, doi:10.1117/2.1200701.0513.
11. Anoikin, E.V.; Sides, P.J. Plasma-activated chemical vapor deposition of bismuth-substituted iron garnets for magneto-optical data storage. *IEEE Transactions on Magnetics* **1995**, *31*, 3239–3241,

doi:10.1109/20.490335.

12. Kang, S.; Yin, S.; Adyam, V.; Li, Q.; Zhu, Y. Bi$_{3}$Fe$_{4}$Ga$_{1}$O$_{12}$ Garnet Properties and Its Application to Ultrafast Switching in the Visible Spectrum. *IEEE Transactions on Magnetics* **2007**, *43*, 3656–3660, doi:10.1109/TMAG.2007.900874.
13. Aichele, T.; Lorenz, A.; Hergt, R.; Görnert, P. Garnet layers prepared by liquid phase epitaxy for microwave and magneto-optical applications – a review. *Crystal Research and Technology* **2003**, *38*, 575–587, doi:10.1002/crat.200310071.
14. Gomi, M.; Tanida, T.; Abe, M. rf sputtering of highly Bi-substituted garnet films on glass substrates for magneto-optic memory. *Journal of Applied Physics* **1985**, *57*, 3888–3890, doi:10.1063/1.334905.
15. Goossens, V.; Wielant, J.; Van Gils, S.; Finsy, R.; Terryn, H. Optical properties of thin iron oxide films on steel. *Surface and Interface Analysis* **2006**, *38*, 489–493, doi:10.1002/sia.2219.
16. van der Zaag, P.J.; Fontijn, W.F.J.; Gaspard, P.; Wolf, R.M.; Brabers, V.A.M.; van de Veerdonk, R.J.M.; van der Heijden, P.A.A. A study of the magneto-optical Kerr spectra of bulk and ultrathin Fe3O4. *Journal of Applied Physics* **1996**, *79*, 5936, doi:10.1063/1.362112.
17. Erenfest Eshenfel'der A., Fizika i tekhnika tsilindricheskikh magnitnykh domenov. Moskva, Mir.: 1983.
18. Kim, Y.H.; Kim, J.S.; Kim, S.I.; Levy, M. Epitaxial Growth and Properties of Bi-Substituted Yttrium-Iron-Garnet Films Grown on (111) Gadolinium-Gallium-Garnet Substrates by Using rf Magnetron Sputtering. *Journal- Korean Physical Society*, **2003**, 43(3):400-405
19. Jongwannasiri, C.; Watanabe, S. Effects of RF Power and Treatment Time on Wettability of Oxygen Plasma-Treated Diamond-like Carbon Thin Films. *International Journal of Chemical Engineering and Applications* **2014**, *5*, 13–16, doi:10.7763/IJCEA.2014.V5.342.
20. Song, B.J.; Hong, K.; Kim, W.-K.; Kim, K.; Kim, S.; Lee, J.-L. Effect of Oxygen Plasma Treatment on Crystal Growth Mode at Pentacene/Ni Interface in Organic Thin-Film Transistors. *The Journal of Physical Chemistry B* **2010**, *114*, 14854–14859, doi:10.1021/jp106364v.
21. Faber, H.; Hirschmann, J.; Klaumünzer, M.; Braunschweig, B.; Peukert, W.; Halik, M. Impact of Oxygen Plasma Treatment on the Device Performance of Zinc Oxide Nanoparticle-Based Thin-Film Transistors. *ACS Applied Materials & Interfaces* **2012**, *4*, 1693–1696, doi:10.1021/am2018223.
22. Vesel, A.; Mozetic, M. Surface functionalization of organic materials by weakly ionized highly dissociated oxygen plasma. *Journal of Physics: Conference Series* **2009**, *162*, 012015, doi:10.1088/1742-6596/162/1/012015.
23. Roh, J.W.; Yang, J.S.; Ok, S.H.; Woo, D.H.; Byun, Y.T.; Jhon, Y.M.; Mizumoto, T.; Lee, W.Y.; Lee, S. Low Temperature O2 Plasma-Assisted Wafer Bonding of InP and a Garnet Crystal for an Optical Waveguide Isolator. *Solid State Phenomena* **2007**, *124–126*, 475–478, doi:10.4028/www.scientific.net/SSP.124-126.475.
24. Mehmood, T.; Kaynak, A.; Dai, X.J.; Kouzani, A.; Magniez, K.; Rubin de Celis, D.; Hurren, C.J.; du Plessis, J. Study of oxygen plasma pre-treatment of polyester fabric for improved polypyrrole adhesion. *Materials Chemistry and Physics* **2014**, *143*, 668–675, doi:10.1016/j.matchemphys.2013.09.052.
25. Bhoi, B.; Mahender, C.; Venkataramani, N.; Aiyar, R.P.R.C.; Prasad, S. Effect of Oxygen Pressure on the Magnetic Properties of Yttrium-Iron-Garnet Thin Films Made by Pulsed Laser Deposition. *IEEE Magnetics Letters* **2016**, *7*, 1–4, doi:10.1109/LMAG.2016.2598720.
26. Yu, D.; Lu, Y.F.; Xu, N.; Sun, J.; Ying, Z.F.; Wu, J.D. Preparation of α-Al2O3 thin films by electron

cyclotron resonance plasma-assisted pulsed laser deposition and heat annealing. *Journal of Vacuum Science & Technology A: Vacuum, Surfaces, and Films* **2008**, *26*, 380–384, doi:10.1116/1.2899569.

27. Nachimuthu, R.K.; Jeffery, R.D.; Martyniuk, M.; Woodward, R.C.; Metaxas, P.J.; Dell, J.M.; Faraone, L. Investigation of Cerium-Substituted Europium Iron Garnets Deposited by Biased Target Ion Beam Deposition. *IEEE Transactions on Magnetics* **2014**, *50*, 1–7, doi:10.1109/TMAG.2014.2331016.
28. Loho, C.; Djenadic, R.; Bruns, M.; Clemens, O.; Hahn, H. Garnet-Type Li 7 La 3 Zr 2 O 12 Solid Electrolyte Thin Films Grown by CO 2 -Laser Assisted CVD for All-Solid-State Batteries. *Journal of The Electrochemical Society* **2017**, *164*, A6131–A6139, doi:10.1149/2.0201701jes.
29. Ma, Q.; Ogino, A.; Matsuda, T.; Nagatsu, M. Defect Control of ZnO Nano-particles Fabricated by Pulsed Nd:YAG Laser Ablation. *Transactions of the Materials Research Society of Japan* **2010**, *35*, 611–615, doi:10.14723/tmrsj.35.611.
30. Kaynak, A.; Mehmood, T.; Dai, X.; Magniez, K.; Kouzani, A. Study of Radio Frequency Plasma Treatment of PVDF Film Using Ar, O2 and (Ar + O2) Gases for Improved Polypyrrole Adhesion. *Materials* **2013**, *6*, 3482–3493, doi:10.3390/ma6083482.
31. Leitenmeier, S.; Heinrich, A.; Lindner, J.K.N.; Stritzker, B. Growth of epitaxial bismuth and gallium substituted lutetium iron garnet films by pulsed laser deposition. *Journal of Applied Physics* **2006**, *99*, 08M704, doi:10.1063/1.2170057.
32. Pandiyaraj, K.N.; Kumar, A.A.; Ramkumar, M.C.; Sachdev, A.; Gopinath, P.; Cools, P.; De Geyter, N.; Morent, R.; Deshmukh, R.R.; Hegde, P.; et al. Influence of non-thermal TiCl4/Ar + O2 plasma-assisted TiOx based coatings on the surface of polypropylene (PP) films for the tailoring of surface properties and cytocompatibility. *Materials Science and Engineering: C* **2016**, *62*, 908–918, doi:10.1016/j.msec.2016.02.042.
33. Christen, H.M.; Ohkubo, I.; Rouleau, C.M.; JellisonJr, G.E.; Puretzky, A.A.; Geohegan, D.B.; Lowndes, D.H. A laser-deposition approach to compositional-spread discovery of materials on conventional sample sizes. *Measurement Science and Technology* **2005**, *16*, 21–31, doi:10.1088/0957-0233/16/1/004.
34. Krumme, J.-P.; David, B.; Doormann, V.; Eckart, R.; Rab, G.; Dossεl, O. Growth, morphology and superconductivity of epitaxial $(RE)_1Ba_2Cl_{13}O_{7-\delta}$ films on $SrTiO_3$ AND $NdGaO_3$. *Substrates*; 1997; Vol. 92;.
35. Nur-E-Alam, M.; Vasiliev, M.; Kotov, V.; Alameh, K. Recent Developments in Magneto-optic Garnet-type Thin-film Materials Synthesis. *Procedia Engineering* **2014**, *76*, 61–73, doi:10.1016/j.proeng.2013.09.248.
36. Nur-E-Alam, M.; Vasiliev, M.; Alameh, K.; Kotov, V.; Demidov, V.; Balabanov, D. YIG: Bi 2 O 3 Nanocomposite Thin Films for Magnetooptic and Microwave Applications. *Journal of Nanomaterials* **2015**, *2015*, 1–6, doi:10.1155/2015/182691.
37. Sun, Y.; Song, Y.-Y.; Chang, H.; Kabatek, M.; Jantz, M.; Schneider, W.; Wu, M.; Schultheiss, H.; Hoffmann, A. Growth and ferromagnetic resonance properties of nanometer-thick yttrium iron garnet films. *Applied Physics Letters* **2012**, *101*, 152405, doi:10.1063/1.4759039.
38. Balabanov, D.E.; Kotov, V.A.; Shavrov, V.G.; Vasiliev, M.; Alameh, K. Magneto-optical methods for analysis of nanothick magnetodielectric films. *Journal of Communications Technology and Electronics* **2017**, *62*, 78–82, doi:10.1134/S106422691701003X.

39. Vasiliev, M.; Alameh, K.; Nur-E-Alam, M. Analysis, Optimization, and characterization of magnetic photonic crystal structures and thin-film material layers. Technologies 2019, 7(3), 49; https://doi.org/10.3390/technologies7030049.